Journal of Sound and Vibration (2003) **259**(3), 605–624
doi:10.1006/jsvi.2002.5111, available online at http://www.idealibrary.com on IDEAL®

DYNAMIC ANALYSIS OF A SPIRAL BEVEL-GEARED ROTOR-BEARING SYSTEM

M. Li and H. Y. Hu

Institute of Vibration Engineering Research, Nanjing University of Aeronautics and Astronautics, 210016 *Nanjing, People's Republic of China. E-mail: Lim@kust.sn.cn*

(*Received* 1 *November* 2001, *and in final form* 8 *April* 2002)

Spiral bevel gears can transmit motion between two rotors, which are commonly perpendicular to each other. In this paper, the dynamic analysis of a spiral bevel-geared rotor-bearing system is studied. Firstly, the constraint equation describing the relationship between the generalized displacements of spiral bevel gear pairs is derived briefly. Then the modelling of coupled axial–lateral–torsional vibration of the rotor system geared by spiral bevel gears is discussed. Finally, the mechanism of coupled vibration of the spiral bevel-geared rotor system is analyzed theoretically and the dynamic behavior of the system is investigated numerically. The conclusions are characterized as follows. The influences of the critical speeds in rigid journal supports, stability threshold speed and unbalanced responses in hydrodynamic journal bearings are not remarkable in comparison with the spur bevel-geared system under the same conditions. However, the critical speeds and stability threshold speed are essentially affected by boundary conditions such as the torsional stiffness, and meanwhile the effect of the unbalanced responses is not prominent under the concerned rotating speeds except that around the resonance peaks. The steady state response due to torsional excitation is also analyzed, and the results show that it cannot be neglected either in the torsional direction or in the lateral and axial directions in the spiral bevel-geared rotor system.

© 2002 Elsevier Science Ltd. All rights reserved.

1. INTRODUCTION

Along with the operating speed of the rotor system trained by gears growing higher in pursuit of high efficiency of machinery, the vibration problems of the system become serious and of increasing concern. Spiral bevel gears are widely used for intersecting rotors to transfer power and motion due to their advantages such as large overlap coefficient, smooth transmission, high rotating speed, low noise, and low sensitivity to assembly errors: e.g., rotorcraft, vehicles, ships and other industrial machinery. In helicopter applications, spiral bevel gears are used in main- and tail-rotor gearboxes to drive the rotors. Although they are of the above benefits to the transmission of the rotor system, some faults of the geared system still exist. For instance, spiral bevel gears in the transmission system of aviation are often damaged due to excess dynamics loads or resonance of the system. However, some researchers tend to look for new gear types or structures to improve the situations, e.g., see, reference [1]. Actually, the transmission system consists of rotors, bearings and bevel gears, and so on. If one of these components such as a rotor or bearing in the system is not suitable for dynamics although the gears are designed very well, the characteristics of the whole system will deteriorate. Thus the perfect dynamic behavior of the whole system is very important. However, hitherto there have

0022-460X/02/$35.00 © 2002 Elsevier Science Ltd. All rights reserved.

been very few studies dealing with dynamic characteristics in the rotor-bearing system geared by spiral bevel gears, and little literature has been published to explain the mechanism of the vibrations of these systems. Hirogaki *et al.* [2] modelled the rotational motion of Oerlikon-type spiral bevel gears by means of virtual cylindrical gears. Their goal was to reduce vibrations of the gear housing. Xu *et al.* [3] analyzed the coupled lateral–torsional vibration behavior of the rotors with the engagement of spiral bevel gears by means of the transfer matrix method, which neglected to consider the relationships of the generalized displacements between two bevel gears. Li *et al.* [4] calculated the critical speed, the unbalanced response, and initial bending response for a miniature engine by the same method. Cardona [5] presents a formulation for describing gear pairs in the three-dimensional analysis of flexible mechanisms. On the other hand, some investigators pay more attention to the characteristics of meshing, dynamic load, teeth strength, noise, etc. in spiral bevel gear itself such as Gleason- and Oerlikon-type spiral bevel gear. For instance, Lewicki *et al.* [1] performed the noise, vibration and tooth strain tests in three different bevel gears. Fang *et al.* [6] developed a mathematical model of the system to predict the dynamic responses and loads on the gears in transmission.

In all of the above investigations, where the characteristics of the bevel gear itself were mainly concerned, there is a lack of extensive dynamic analysis, such as the stability, steady state response, etc. for the whole rotor-bearing system geared by spiral bevel gears. However, it is more exigent when the system tends to large scale, high speed, heavy load, etc. On the other hand, more attention has been paid recently to the noise from the gearbox of the rotor system, which is closely related to the vibration. Harris [7] analyzed the vibration of a right-angle drive, bevel-pinion-type gearbox, and found that the bevel gear on the intermediate shaft was the major noise contributor. Hence the investigation of the dynamics of the rotor system geared by bevel gears is significant.

In this paper, we continue to discuss the dynamics of the coupled axial–lateral–torsional vibration of the rotor-bearing system geared by spiral bevel gears based on the literature [8]. Firstly, the dynamic model is developed to suit the perpendicularly spiral bevel-geared rotor-bearing system, and then the mechanism of coupled vibrations of the system is analyzed in theory. Finally, we analyze the dynamic characteristics of the system in some cases.

2. EQUATIONS OF MOTION

2.1. CONSTRAINT EQUATION

Bevel gear teeth are higher element kinematic pairs, with constrained motion, that engage with slide contact. The tooth surface of a bevel gear is formed by a family of spherical involute curves for straight bevels [9]. Therefore, the inherent generalized displacements between a pair of bevel gears are complex. Figure 1(a) shows a rotor system geared by a bevel gear pair, whose transmission can be simplified by a virtual cylindrical gear pair shown in Figure 1(b).

In this analysis, the major assumptions, such as neglecting the errors and deformations of gear teeth, are the same as in reference [8], so that the following relationship between two gears is also satisfied:

$$x_{e1}\sin\alpha + y_{e1}\cos\alpha + r_{b1}\theta_1 = x_{e2}\sin\alpha + y_{e2}\cos\alpha + r_{b2}\theta_2, \tag{1}$$

where α is the pressure angle of the gear, and r_{b1} and r_{b2} are the radii of base circles of the two virtual cylindrical gears.

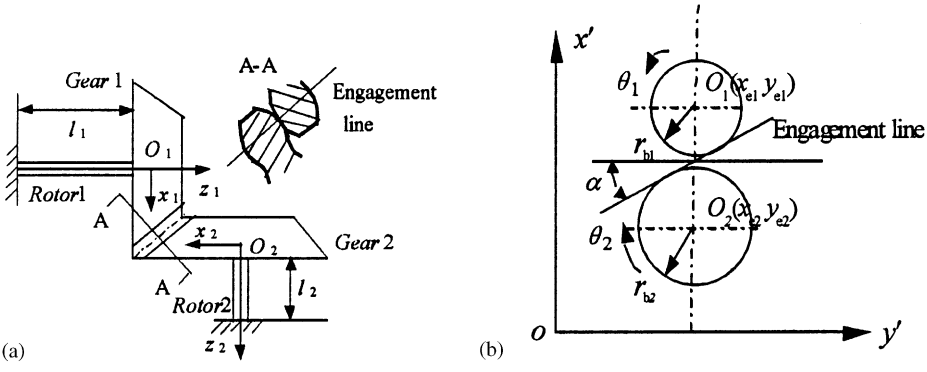

Figure 1. A simple rotor system geared by bevel gears and their virtual cylindrical gears of bevel gears.

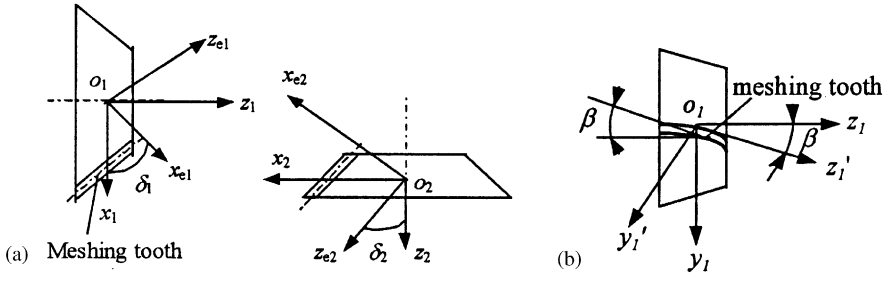

Figure 2. A pair of spiral bevel gears and a spiral profile tooth.

As shown in Figure 2(a), the straight bevel motion described in the co-ordinate frame $ox_{ei}y_{ei}z_{ei}$ can be determined from

$$\begin{Bmatrix} x_{ei} \\ y_{ei} \\ z_{ei} \end{Bmatrix} = \begin{bmatrix} \cos\delta_i & 0 & \sin\delta_i \\ 0 & 1 & 0 \\ -\sin\delta_i & 0 & \cos\delta_i \end{bmatrix} \begin{Bmatrix} x_i' \\ y_i' \\ z_i' \end{Bmatrix}, \tag{2}$$

where $\delta_i = \delta_1, -\delta_2$ $(i = 1, 2)$ are the pitch cone angles and x_i, y_i, z_i $(i = 1, 2)$ are the co-ordinates of the two gear centers.

Spiral bevel gears have curved oblique teeth on which contact begins gradually and continues smoothly from end to end. They mesh with a rolling contact similar to straight bevels. The tooth of the spiral bevel gear shown in Figure 2(b), which inclines away from the axis in the counterclockwise direction, is called left-handed in the Gleason-type gear. Furthermore, the mating member, which is always the opposite of the former, is called right-handed. Now for simplicity, we suppose that the points of contact on adjacent teeth are in their mid-width; then a co-ordinate system transform is needed, i.e.,

$$\begin{Bmatrix} x_i' \\ y_i' \\ z_i' \end{Bmatrix} = \begin{bmatrix} 1 & 0 & 0 \\ 0 & \cos\beta_i & -\sin\beta_i \\ 0 & \sin\beta_i & \cos\beta_i \end{bmatrix} \begin{Bmatrix} x_i \\ y_i \\ z_i \end{Bmatrix}, \tag{3}$$

where the mid-spiral angles of the gears $\beta_i = \beta, -\beta$ $(i = 1, 2)$.

Substituting equation (3) into expression (2), and then into equation (1), the constraint equation of small perturbations of motion reads

$$x_1 \sin\alpha\cos\delta_1 + y_1(\cos\alpha\cos\beta + \sin\alpha\sin\beta\sin\delta_1) - z_1(\cos\alpha\sin\beta - \sin\alpha\cos\beta\sin\delta_1) + \theta_1 r_{b1} = x_2\sin\alpha\cos\delta_2 + y_2(\cos\alpha\cos\beta + \sin\alpha\sin\beta\sin\delta_2) + z_2(\cos\alpha\sin\beta - \sin\alpha\cos\beta\sin\delta_2) + \theta_2 r_{b2}. \tag{4}$$

The above equation can be written in simplified form as

$$a_1x_1 + b_1y_1 + c_1z_1 + d_1\theta_1 = a_2x_2 + b_2y_2 + c_2z_2 + d_2\theta_2, \tag{5}$$

where the parameters a_i, b_i, c_i, d_i $(i = 1, 2)$ are only related to the geometry of the spiral teeth profiles as shown in the following. Thus, the parameters in equation (5) become

$$\begin{aligned} &a_1 = \sin\alpha\cos\delta_1, \quad a_2 = \sin\alpha\cos\delta_2,\\ &b_1 = \cos\alpha\cos\beta + \sin\alpha\sin\beta\sin\delta_1, \quad b_2 = \cos\alpha\cos\beta + \sin\alpha\sin\beta\sin\delta_2,\\ &c_1 = -(\cos\alpha\sin\beta - \sin\alpha\cos\beta\sin\delta_1), \quad c_2 = \cos\alpha\sin\beta - \sin\alpha\cos\beta\sin\delta_2,\\ &d_1 = r_{b1}, \quad d_2 = r_{b2}, \end{aligned} \tag{6}$$

2.2. EQUATIONS OF MOTION

Equation (4) or (5) is a kinetic constraint condition of two meshing bevel gears in the system. It indicates a coupling among the axial, lateral and torsional degrees of freedom. For the development of governing equations of these systems under complex constraint conditions, there are some advantages on Lagrange's equation, which are as follows:

$$\frac{\mathrm{d}}{\mathrm{d}t}\left(\frac{\partial T}{\partial \dot{q}}\right) - \frac{\partial T}{\partial q} + \frac{\partial U}{\partial q} = Q, \tag{7}$$

where T, U, Q and q are the kinetic energy, potential energy, generalized forces and generalized co-ordinates of the system respectively. Based on equations (5) and (7), the equations of motion of the system can be derived conveniently. A simple example for the development of equations of motion of the system is given in detail in Appendix A.

For a practical system, we can write its differential equations as

$$\mathbf{M}\ddot{\mathbf{q}} + (\mathbf{G} + \mathbf{C})\dot{\mathbf{q}} + \mathbf{K}\mathbf{q} = \mathbf{Q}, \tag{8}$$

where $\mathbf{M}$, $\mathbf{G}$, $\mathbf{C}$ and $\mathbf{K}$ are the generalized mass, gyroscopic, damping and generalized stiffness matrices, and $\mathbf{Q}$ and $\mathbf{q}$ are the generalized force and displacement vectors respectively. In general, $\mathbf{Q}$ is composed of unbalanced forces, exciting torque, etc. in geared rotor dynamics.

Although the presented model is developed for the spiral bevel-geared rotor-bearing system, it can also be used in the corresponding system geared by zero1, straight bevel gears, For the hypoid geared system, a further co-ordinate transform between gear and pinion may be needed.

3. MECHANISM OF THE COUPLED VIBRATION

In order to clarify the mechanism of coupled vibration of the bevel-geared system, we consider the system as shown in Figure 1(a), which is composed of two same massless rotors and spiral bevel gears. The rotors are supported by rigid bearings. Ignoring the motion in the x direction (horizontal), constraint equation (7) is haply of the

following form:

$$y_1 + z_1 + r_b\theta_1 = y_2 + z_2 + r_b\theta_2. \tag{9}$$

Although the above equation is not precise, it implies the relationship among the lateral, axial and torsional direction. In this way, a system of 5 degrees of freedom can be obtained while neglecting the gyroscopic effect and damping forces (or moments). Then the equation of motion can be derived in terms of Appendix A; furthermore, if the polar moments of inertia of the gear are approximately equal to $J = mr_b^2/2$, and $k = k_t/r_b^2$, then it reads as

$$\mathbf{M}\ddot{\mathbf{q}} + \mathbf{K}\mathbf{q} = 0, \tag{10}$$

where

$$\mathbf{M} = \frac{m}{2}\begin{bmatrix} 3 & 1 & r_b & -1 & -1 \\ & 3 & r_b & -1 & -1 \\ & & 2r_b^2 & -r_b & -r_b \\ & symm. & & 3 & 1 \\ & & & & 3 \end{bmatrix}, \tag{11}$$

$$\mathbf{K} = \begin{bmatrix} k_y + k & k & kr_b & -k & -k \\ & k_a + k & kr_b & -k & -k \\ & & 2kr_b^2 & -kr_b & -kr_b \\ & symm. & & k_y + k & k \\ & & & & k_a + k \end{bmatrix}, \tag{12}$$

$$\mathbf{q} = [y_1 \;\; z_1 \;\; \theta_1 \;\; y_2 \;\; z_2]^{\mathrm{T}}, \tag{13}$$

in which m is the mass of gears, and k_y, k_a, k_t are the stiffness of the rotor in the lateral, axial and torsional directions respectively.

In the matrices $\mathbf{M}$ and $\mathbf{K}$, there exist coupled terms among the $\ddot{y}_1 \;\; \ddot{z}_1 \;\; \ddot{\theta}_1 \;\; \ddot{y}_2 \;\; \ddot{z}_2$ and $y_1 \;\; z_1 \;\; \theta_1 \;\; y_2 \;\; z_2$ respectively. That is, the coupled terms only relate to the geometric parameters of bevel gears and the rotor system. Hence, the lateral, torsional and axial vibrations are coupled with each other. In practice, equation (9) suggests the coupled relationship, which is the source connecting the lateral, torsional and axial vibrations.

The generalized eigenvalue problem that is from equation (10), that is, the natural frequencies and their modes on dynamics, can be solved theoretically. The following results are calculated by using Maple V:

$$\omega_1^2 = k_t/J \quad \text{torsional mode},$$

$$\omega_2^2 = k_y/m \quad \text{lateral mode},$$

$$\omega_3^2 = k_z/m \quad \text{axial mode},$$

$\omega_{4,5}^2 = \frac{1}{8}(2\omega_1^2 + 3\omega_2^2 + 3\omega_3^2 \mp \sqrt{4\omega_1^4 + 9\omega_2^4 + 9\omega_3^4 - 4\omega_1^2\omega_2^2 - 4\omega_1^2\omega_3^2 - 14\omega_2^2\omega_3^2})$ coupled modes, where $\omega_1, \omega_2, \ldots$ are all natural frequencies of the system.

In the above five modes, the first three are the pure torsional, lateral and axial ones, respectively, which can be obtained by the traditional method. Based on this method, the torsional natural frequencies of the composite rotor train and, in addition, the lateral and axial ones of the individual rotors are calculated. However, the last two modes are coupled in the torsional, lateral and axial directions, which cannot be analyzed by the traditional

method. If constrainedly using on it, some important dynamic characteristics of this system such as ω_4, ω_5 will be lost. However, the above results show that ω_4 and ω_5 are related to the parameters of the system in all three directions, and coupled not only in values of natural frequencies but also in their modes. The coupled modes should be concerned more because they can be excited by different directions; for example, the lateral and axial responses may be from the torque exciter. Then, the probability of the resonance for the high-speed rotor system geared by spiral bevel gears is increased. The further analysis is discussed in the following section.

4. DIGITAL SIMULATION

In the above theoretical analysis, some conditions are ignored such as the gyroscopic effect of the disks, damping of the bearings, etc. Generally for a practical system, these cannot be neglected, so that digital simulation is necessary. In order to study the critical speeds, the stability threshold speed, etc. of the rotor-bearing system geared by spiral bevel gears, an example is given in this section. Figure 3 shows a system in which each rotor is laterally supported by two journal bearings. These are two identical 360° cylindrical bearings at nodes 1 and 3, and two 5-pad tilting-pad bearings at nodes 6 and 8 respectively. A rigid axial support is located at node 1 to constrain the axial rigid motion. The eight coefficients of bearings are calculated based on the short-bearing assumption. The geometric or structure parameters of the system are shown in Table 1. In the system each rotor is discretized into four nodes, that is, no. 1–4 nodes represent rotor 1 and 5–8 represent rotor 2 as shown in Figure 3. There are 47 degrees of freedom in total.

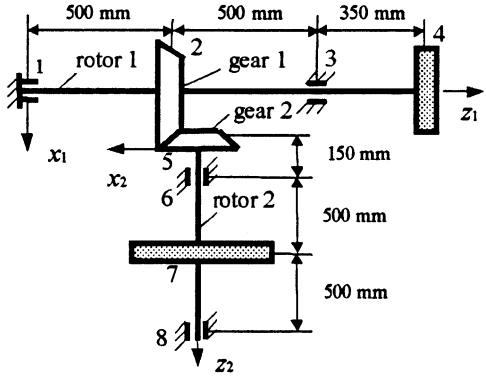

Figure 3. A rotor-bearing system geared by spiral bevel gears.

TABLE 1

The system parameters

Bearing	$D_0 = 100\,\text{mm}$, $L_0/D_0 = 0{\cdot}5$, $\psi_0 = 0{\cdot}002$, $\mu = 0{\cdot}0221\,\text{N s/m}^2$
Mass of disks and gears	$m_2 = 600\,\text{kg}$, $m_4 = 300\,\text{kg}$, $m_5 = 40\,\text{kg}$, $m_7 = 600\,\text{kg}$
Moments of inertia	$J_2^d = 15\,\text{kg m}^2$, $J_4^d = 12\,\text{kg m}^2$, $J_5^d = 0{\cdot}05\,\text{kg m}^2$, $J_7^d = 15\,\text{kg m}^2$, $J_2^z = 25\,\text{kg m}^2$, $J_4^z = 20\,\text{kg m}^2$, $J_5^z = 0{\cdot}072\,\text{kg m}^2$, $J_7^z = 25\,\text{kg m}^2$
Spiral bevel gears	$\alpha = 20°$, $\delta_1 = 70°$, $\delta_2 = 20°$, $r_{b1} = 300\,\text{mm}$, $r_{b2} = 100\,\text{mm}$
Rotors	$d = 100\,\text{mm}$, $E = 206\,\text{GN/m}^2$, $G = 78\,\text{GN/m}^2$

When the generalized force $\mathbf{Q} = \mathbf{0}$, equation (8) governs the free vibration of the system, the corresponding eigenvalue problem can be solved numerically by using the generalized inverse iteration method in reference [10], and when $\mathbf{Q} \neq \mathbf{0}$, the corresponding forced responses can be obtained in terms of the following approach.

Let the external excited forces have the forms

$$\mathbf{Q} = (\mathbf{Q}_R + \mathrm{j}\mathbf{Q}_I)\, \mathrm{e}^{\mathrm{j}N\Omega t}, \tag{14}$$

where $\mathbf{Q}_R$ and $\mathbf{Q}_I$ represent the real and imaginary parts of the force, respectively, and N is an integer which may be equal to the teeth number of the gears or order number of the cyclic speed variation in the geared rotor system. When $N = 1$, the frequency of external excited force is synchronous with speed Ω. Consequently, the corresponding responses are

$$\mathbf{q} = (\mathbf{q}_{R0} + \mathrm{j}\mathbf{q}_{I0})\, \mathrm{e}^{\mathrm{j}N\Omega t}, \tag{15}$$

in which $\mathbf{q}_{R0}$ and $\mathbf{q}_{I0}$ also represent the real and imaginary parts of the responses respectively. Substituting equations (14) and (15) into equation (8), the amplitudes of the responses read as

$$\begin{bmatrix} \mathbf{K} - \mathbf{M}N^2\Omega^2 & -(\mathbf{G} + \mathbf{C})N\Omega \\ (\mathbf{G} + \mathbf{C})N\Omega & \mathbf{K} - \mathbf{M}N^2\Omega^2 \end{bmatrix} \begin{Bmatrix} \mathbf{q}_{R0} \\ \mathbf{q}_{I0} \end{Bmatrix} = \begin{Bmatrix} \mathbf{Q}_R \\ \mathbf{Q}_I \end{Bmatrix}. \tag{16}$$

The responses of vibration, that is, the solution of the above linear algebraic equations, can be solved by Gaussian elimination. Then the amplitudes of their responses become

$$\mathbf{A} = \sqrt{\mathbf{q}_{R0}^2 + \mathbf{q}_{I0}^2}. \tag{17}$$

4.1. INFLUENCE OF DYNAMICS BY SPIRAL SPIRAL ANGLE

The analysis on dynamics which includes the critical speeds of rigid supports, threshold stability speed on bearing supports and its responses due to external excitations is the major subject in the geared rotor system. In this section, we emphatically discuss the influence on dynamics by the spiral angle β, which is the main geometric parameter of the spiral bevel gear.

Table 2 depicts the influence of the spiral angle β on the critical speeds of the rigidly supported rotor system. The results indicate that the critical speeds vary a little. In the table, the vibration components of the speeds from the first to the seventh are mainly from the lateral and torsional directions, and that is very small from the axial. But the 11th speed is almost contributed by the axial. Table 3 shows the influence of β on the stability threshold speed of the system supported by oil film bearings. The results indicate that the threshold speed changes a little.

In the geared rotor system, there are several external excitations acting on the system, in which the unbalances of rotors or disks and the torsional excitation are the major ones, so

TABLE 2

Critical speeds of the rigidly supported rotor system (r.p.m.)

Spiral angle (deg)	First	Second	Third	Fourth	Fifth	Sixth	Seventh	11th
$\beta = 0$	1399	1743	2265	2694	2706	3347	3501	16 086
$\beta = 20$	1393	1741	2276	2694	2704	3335	3500	16 074
$\beta = 35$	1413	1785	2282	2694	2703	3347	3500	16 085

that in this section we pay more attention to the steady state responses of the system due to them. Tables 4–6 give the lateral, axial and torsional amplitudes at the four oil film bearings at the rotating speed 2800 r.p.m. of rotor 1 and the offset of unbalance to be 0·01 mm at gear on rotor 1. In these three cases, the variations of the lateral and torsional responses are not large, and the vibration level of the axial one is small although its variation is remarkable. Thus we can conclude that the influences of the spiral angle of bevel gears to the unbalanced response are not sensitive.

The above results reveal that if we want to change the dynamic behavior such as critical speeds, stability and unbalanced response of the system, the alternation of the spiral angle β is not very efficient although it is available in the teeth stress, smooth transmission, low noise, etc. That is, for the same rotor-bearing system, whether geared by spiral bevel gears or spur ones or zerol ones, the variation of its dynamic behavior is not large.

TABLE 3

Stability threshold speed (r.p.m.)

$\beta = 0^\circ$	$\beta = 20^\circ$	$\beta = 35^\circ$
3041	2984	3038

TABLE 4

Lateral amplitudes at the four bearings (mm)

Bearing no.	$\beta = 0^\circ$	$\beta = 20^\circ$	$\beta = 35^\circ$
1	$0{\cdot}108 \times 10^{-1}$	$0{\cdot}109 \times 10^{-1}$	$0{\cdot}109 \times 10^{-1}$
2	$0{\cdot}137 \times 10^{-1}$	$0{\cdot}136 \times 10^{-1}$	$0{\cdot}136 \times 10^{-1}$
3	$0{\cdot}167 \times 10^{-3}$	$0{\cdot}179 \times 10^{-3}$	$0{\cdot}161 \times 10^{-3}$
4	$0{\cdot}285 \times 10^{-3}$	$0{\cdot}298 \times 10^{-3}$	$0{\cdot}265 \times 10^{-3}$

TABLE 5

Axial amplitudes at the four bearings (mm)

Bearing no.	$\beta = 0^\circ$	$\beta = 20^\circ$	$\beta = 35^\circ$
1	0·0	0·0	0·0
2	$0{\cdot}262 \times 10^{-5}$	$0{\cdot}169 \times 10^{-6}$	$0{\cdot}228 \times 10^{-5}$
3	$0{\cdot}528 \times 10^{-4}$	$0{\cdot}105 \times 10^{-3}$	$0{\cdot}202 \times 10^{-3}$
4	$0{\cdot}536 \times 10^{-4}$	$0{\cdot}107 \times 10^{-3}$	$0{\cdot}205 \times 10^{-3}$

TABLE 6

Torsional amplitudes at the four bearings (rad)

Bearing no.	$\beta = 0^\circ$	$\beta = 20^\circ$	$\beta = 35^\circ$
1	$0{\cdot}320 \times 10^{-4}$	$0{\cdot}342 \times 10^{-4}$	$0{\cdot}325 \times 10^{-4}$
2	$0{\cdot}777 \times 10^{-5}$	$0{\cdot}833 \times 10^{-5}$	$0{\cdot}790 \times 10^{-5}$
3	$0{\cdot}485 \times 10^{-6}$	$0{\cdot}519 \times 10^{-6}$	$0{\cdot}491 \times 10^{-6}$
4	$0{\cdot}873 \times 10^{-5}$	$0{\cdot}126 \times 10^{-5}$	$0{\cdot}119 \times 10^{-5}$

For the spiral bevel-geared rotor system, because of the coupling in the axial, lateral and torsional directions, their responses can be evoked by excitation from each direction. In the following, we emphasize analyzing the responses due to torsional excitation. The torsional excitation in this kind of system may be generated by the engine, propeller, other auxiliary systems, etc., which can be represented as

$$M = M_0 \sin n\Omega t, \tag{18}$$

where M_0 is the exciting torque amplitude which may be constant or changeable, n the order number of the cyclic speed variation, Ω the angular frequency of the rotor, and t the time. Rao *et al.* [11] discussed the transient lateral response due to sudden torsional excitation in the parallel axis geared rotor system, which was produced by short circuiting torque. In this paper, we suppose that the exciting torque amplitude M_0 is a constant, and the mean value is $M_0 = 100{\cdot}0\,\mathrm{N\,m}$ which acts on bevel gear 1 as well as $n = 1$. In practice, the level of this value may be various in different machinery, so that the actual one is unknown. Fortunately, the principle of superposition is valid on linear dynamics, and can be used in the calculation. Tables 7–9 depict the steady state responses in the lateral, axial and torsional directions at the four oil film bearings at the rotating speed of 2800 r.p.m. of rotor 1. From these tables, we can find that the torsional excitation, which may excite the torsional response that is not large, can evoke sizeable responses not only in the lateral

TABLE 7

Lateral amplitudes at the four bearings (mm)

Bearing no.	$\beta = 0^\circ$	$\beta = 20^\circ$	$\beta = 35^\circ$
1	$0{\cdot}280 \times 10^{-2}$	$0{\cdot}294 \times 10^{-2}$	$0{\cdot}275 \times 10^{-2}$
2	$0{\cdot}124 \times 10^{-2}$	$0{\cdot}134 \times 10^{-2}$	$0{\cdot}132 \times 10^{-2}$
3	$0{\cdot}230 \times 10^{-2}$	$0{\cdot}230 \times 10^{-2}$	$0{\cdot}216 \times 10^{-2}$
4	$0{\cdot}395 \times 10^{-2}$	$0{\cdot}388 \times 10^{-2}$	$0{\cdot}361 \times 10^{-2}$

TABLE 8

Axial amplitudes at the four bearings (mm)

Bearing no.	$\beta = 0^\circ$	$\beta = 20^\circ$	$\beta = 35^\circ$
1	0·0	0·0	0·0
2	$0{\cdot}355 \times 10^{-4}$	$0{\cdot}214 \times 10^{-5}$	$0{\cdot}302 \times 10^{-3}$
3	$0{\cdot}724 \times 10^{-3}$	$0{\cdot}131 \times 10^{-2}$	$0{\cdot}272 \times 10^{-2}$
4	$0{\cdot}735 \times 10^{-3}$	$0{\cdot}133 \times 10^{-2}$	$0{\cdot}276 \times 10^{-2}$

TABLE 9

Torsional amplitudes at the four bearings (rad)

Bearing no.	$\beta = 0^\circ$	$\beta = 20^\circ$	$\beta = 35^\circ$
1	$0{\cdot}255 \times 10^{-4}$	$0{\cdot}255 \times 10^{-4}$	$0{\cdot}215 \times 10^{-4}$
2	$0{\cdot}595 \times 10^{-5}$	$0{\cdot}619 \times 10^{-5}$	$0{\cdot}522 \times 10^{-5}$
3	$0{\cdot}637 \times 10^{-5}$	$0{\cdot}637 \times 10^{-5}$	$0{\cdot}628 \times 10^{-5}$
4	$0{\cdot}161 \times 10^{-4}$	$0{\cdot}160 \times 10^{-4}$	$0{\cdot}160 \times 10^{-4}$

direction but also in the axial one. This result cases the difficult problem in vibration control of the system. That is, while restraining the unbalances of rotors and disks, we must control the amplitudes of torsional excitation. Although it can satisfy the standard of torsional response, it can also exceed the criterion of the lateral one. The tables also show that the largest responses in the lateral and axial directions are on the bearing 4 of rotor 2 notwithstanding the torsional excitation is directly acting on rotor 1, and the axial one is very sensitive to the spiral angle.

4.2. EFFECT ON DYNAMICS BY BOUNDARY CONDITIONS

In the above analysis, it is assumed that the axial support is rigid, i.e., the axial vibration is only due to the deformation of the rotor. In this section, we analyze the case when the axial as well as torsional supports are flexible. Now we suppose that node 1 on rotor 1 and node 8 on rotor 2 are constrained by axial and torsional springs whose stiffness coefficients are k_a and k_t, respectively, as shown in Figure 4. In general, the axial stiffness k_a may be produced by thrust bearings and the torsional stiffness k_t can be brought about by an additional shaft which connects with another structure or subsystem. About modelling of this system, the developing process is similar to that discussed in section 2; k_a and k_t are only added to the corresponding terms in the potential energy. Here we neglect it.

In Table 10, the effects on critical speeds are given in different k_a and k_t, and the modes under the condition $k_a = 1{\cdot}0 \times 10^6$ N/m, $k_t = 0{\cdot}0$ N m are shown in Figure 5, in which the

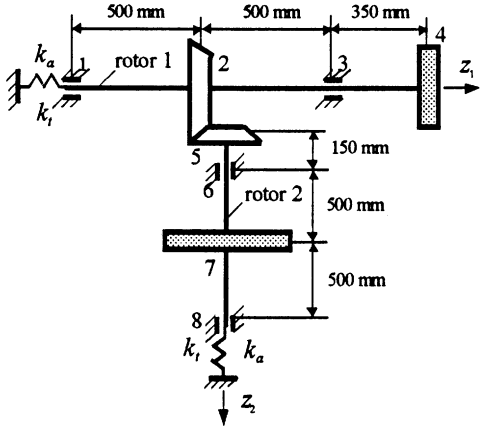

Figure 4. A rotor-bearing system geared by bevel gears.

TABLE 10

Variations of critical speeds versus torsional and axial stiffness (r.p.m.)

k_a (N/m)	k_t (N m)	First	Second	Third	Fourth	Fifth	Sixth	Seventh	Eighth	Ninth
$1{\cdot}0 \times 10^5$	0·0	98	119	1406	1758	2268	2694	2703	3349	—
$1{\cdot}0 \times 10^6$	0·0	310	374	1407	1759	2268	2694	2704	3349	—
$1{\cdot}0 \times 10^7$	0·0	972	1184	1414	1767	2270	2694	2704	3349	—
0·0	$1{\cdot}0 \times 10^6$	244	1343	1477	1849	2288	2696	2732	3388	—
$1{\cdot}0 \times 10^6$	$1{\cdot}0 \times 10^6$	360	410	1343	1478	1849	2289	2696	2732	3388

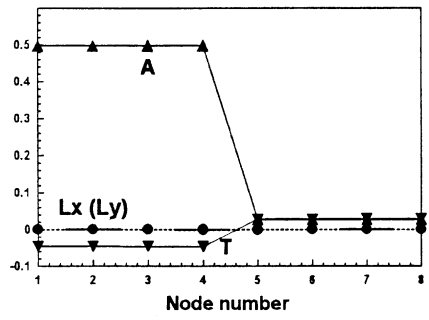

(a) 310 (r.p.m)

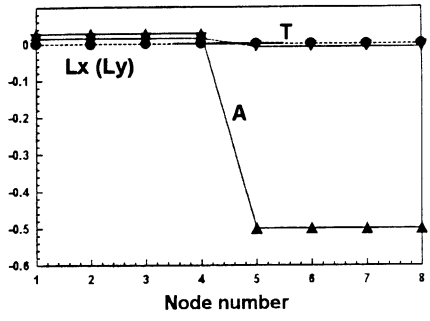

(b) 374 (r.p.m)

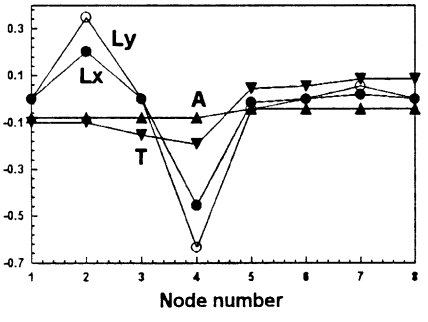

(c) 1407 (r.p.m)

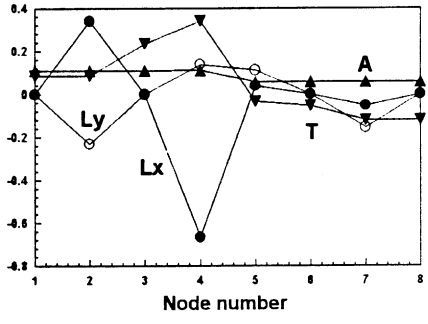

(d) 1759 (r.p.m)

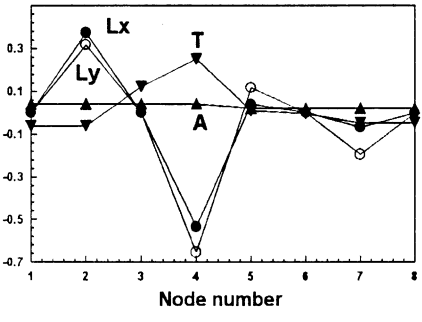

(e) 2268 (r.p.m)

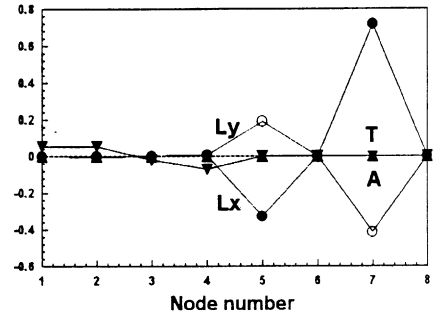

(f) 2694 (r.p.m)

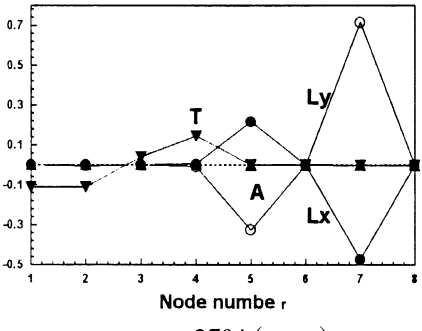

(g) 2704 (r.p.m)

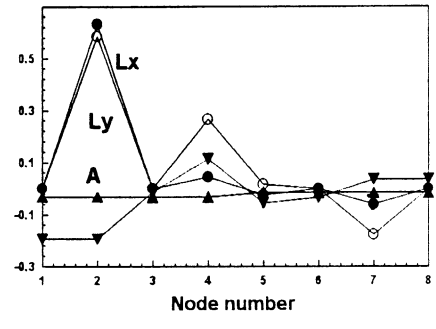

(h) 3349 (r.p.m)

Figure 5. Mode shapes of the rigidly supported system. (a) 310, (b) 374, (c) 1407, (d) 1759, (e) 2268, (f) 2694, (g) 2704, (h) 3349 r.p.m. $k_a = 1{\cdot}0 \times 10^6$ N/m, $k_t = 0{\cdot}0$ N m: —●—, L_x — lateral displacement in the x direction; —○—, L_y — lateral displacement in the y direction; —▲—, A — axial direction; —▼—, T — torsional direction.

horizontal axis represents the node number of the rotors (1–4 as rotor 1 and 5–8 as rotor 2) and the vertical axis the dimensionless generalized displacements. The following conclusions can be drawn from the table and the Figure (1) If only two axial supports are added, two additional lower critical speeds appear, at which the axial vibrations predominate. The first one corresponds to the axial translation of rotor 1, while the second one to rotor 2. The axial deformations of rotors are very small. (2) If only two torsional springs are added, two additional lower critical speeds appear, at which the axial and

TABLE 11

Stability threshold speed of the system on oil film bearings (r.p.m.)

k_t (N m)	k_a (N/m)			
	0	$1{\cdot}0 \times 10^5$	$1{\cdot}0 \times 10^6$	$1{\cdot}0 \times 10^7$
0	—	3059	3068	3087
$1{\cdot}0 \times 10^5$	3089	3090	3093	3113
$1{\cdot}0 \times 10^6$	2921	2921	2920	2916
$1{\cdot}0 \times 10^7$	3209	3209	3210	3215

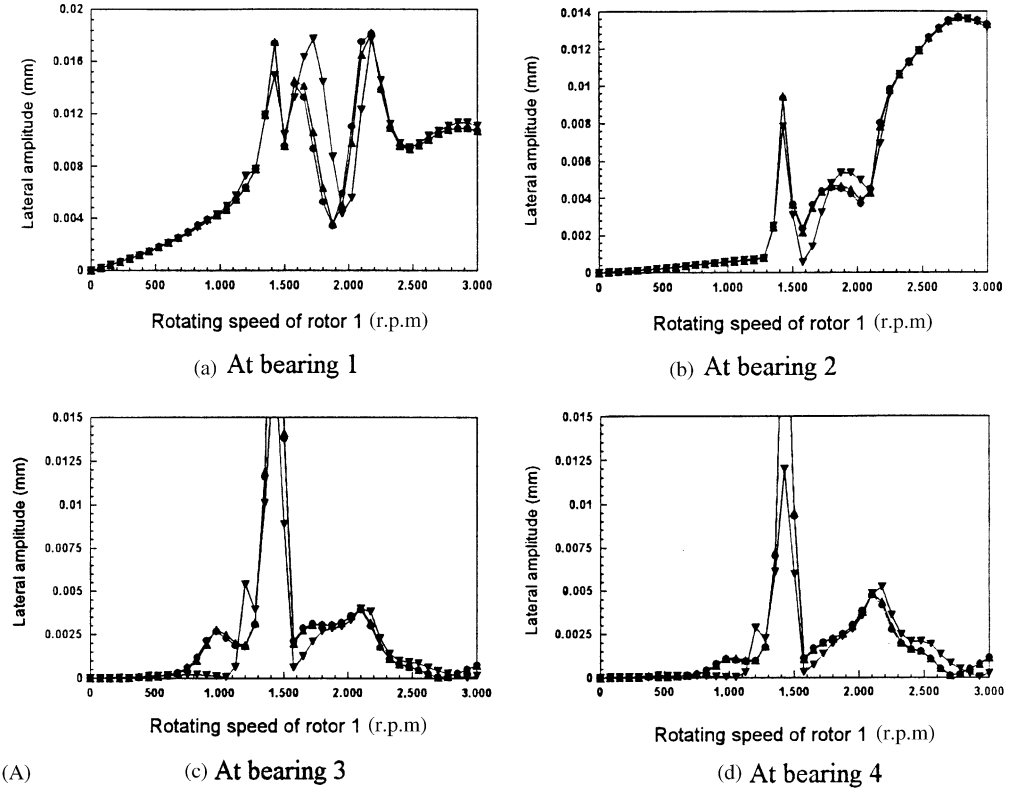

Figure 6. (A) Unbalanced response of the four bearings in the lateral direction: (a) at bearing 1, (b) at bearing 2, (c) at bearing 3, (d) at bearing 4. (B) Unbalanced response of the four bearings in the axial direction: (a) at bearing 1, (b) at bearing 2, (c) at bearing 3, (d) at bearing 4. (C) Unbalanced response of the four bearings in the torsional direction: (a) at bearing 1, (b) at bearing 2, (c) at bearing 3, (d) at bearing 4. —●—, $k_a \to \infty$ N/m, $k_t = 0{\cdot}0$ N m; —▲—, $k_a = 1{\cdot}0 \times 10^6$ N/m, $k_t = 0{\cdot}0$ N m; —▼—, $k_a = 1{\cdot}0 \times 10^6$ N/m, $k_t = 1{\cdot}0 \times 10^6$ N/m.

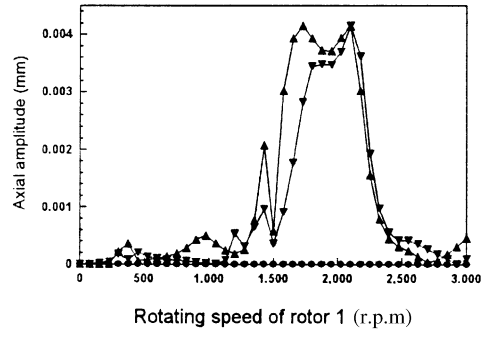

(a) At bearing 1

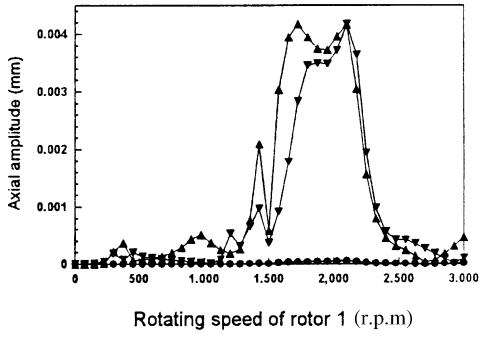

(b) At bearing 2

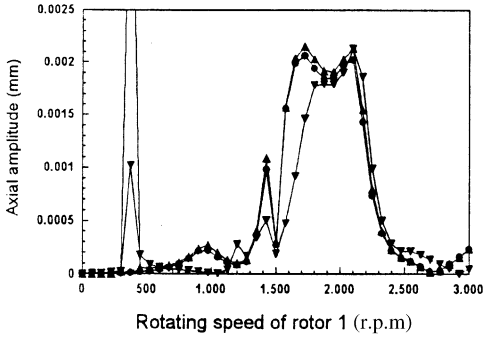

(B) (c) At bearing 3

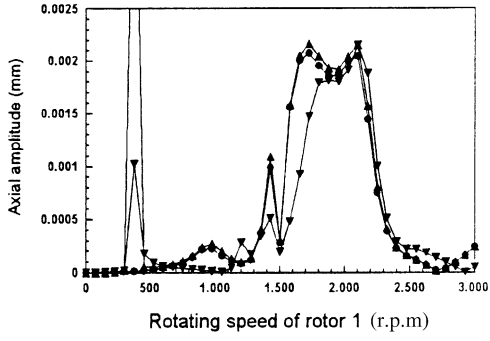

(d) At bearing 4

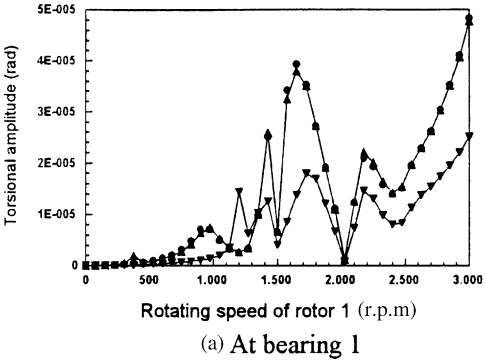

(a) At bearing 1

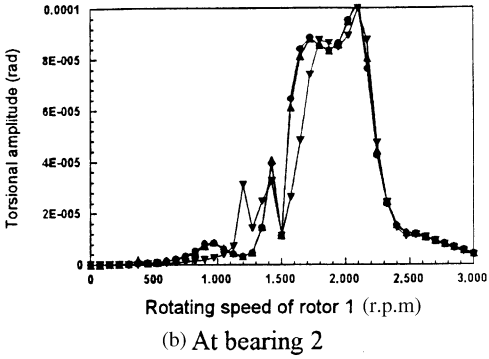

(b) At bearing 2

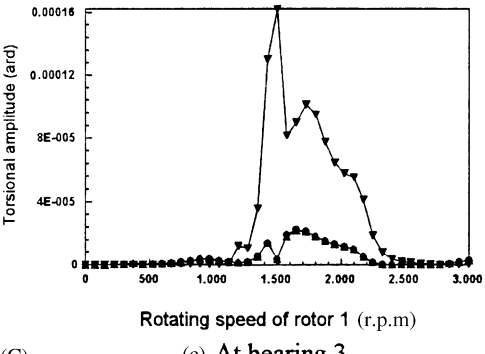

(C) (c) At bearing 3

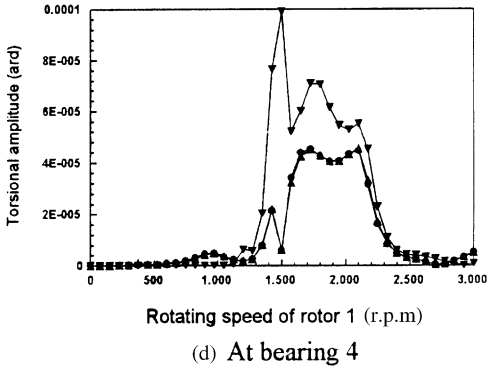

(d) At bearing 4

Figure 6. Continued.

torsional vibrations predominate. (3) If two axial supports and two torsional springs are added, three additional lower critical speeds appear. The axial vibration predominates at the first one (360 r.p.m.). The axial and the torsional vibrations predominate at the second one (410 r.p.m.). The torsional vibration is dominant at the third one (1334 r.p.m.). (4) In addition, the other critical speeds vary to some extent. The stronger the axial or torsional vibration, the greater the variation of the corresponding critical speed.

Table 11 depicts the variations of the stability threshold speed of the system on oil film journal bearings under the different values of k_a and k_t. From this table, we can conclude that the stability threshold is insensitive to the axial stiffness, but is sensitive to the torsional stiffness.

Figure 6 shows the variations of the unbalanced lateral, axial and torsional responses at journal bearings versus the rotating speed when the offset of unbalance is supposed to be 0·01 mm and at the bevel gear on rotor 1. Taking one with another, the responses in the three directions are largely affected by axial stiffness k_a and torsional stiffness k_t around the resonance peaks, and the the speed of 2800 r.p.m. of rotor 1 the effects are decreased consumedly. The figure also indicates that the axial and torsional responses are influenced more than the lateral one by them in the coupled vibration.

Figure 7 reveals the variations of the unbalanced lateral, axial, and torsional responses at four bearings versus the rotating speed due to the torsional excitation which is

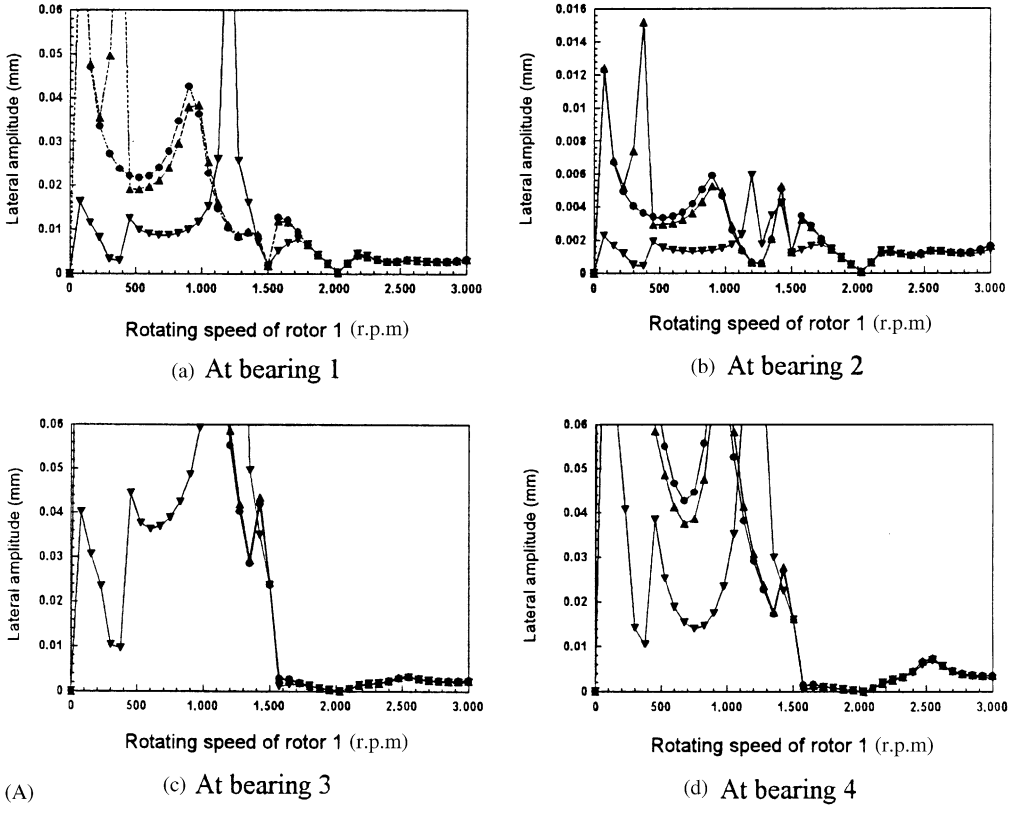

Figure 7. (A) The response of the four bearings in the lateral direction: (a) at bearing 1, (b) at bearing 2, (c) at bearing 3, (d) at bearing 4. (B) The response of the four bearings in the axial direction: (a) at bearing 1, (b) at bearing 2, (c) at bearing 3, (d) at bearing 4. (C) The response of the four bearings in the axial direction: (a) at bearing 1, (b) at bearing 2, (c) at bearing 3, (d) at bearing 4. —●—, $k_a \to \infty$ N/m, $k_t = 0{\cdot}0$ N m; —▲—, $k_z = 1{\cdot}0 \times 10^6$ N/m, $k_t = 0{\cdot}0$ N m; —▼—, $k_a = 1{\cdot}0 \times 10^6$ N/m, $k_t = 1{\cdot}0 \times 10^6$ N/m.

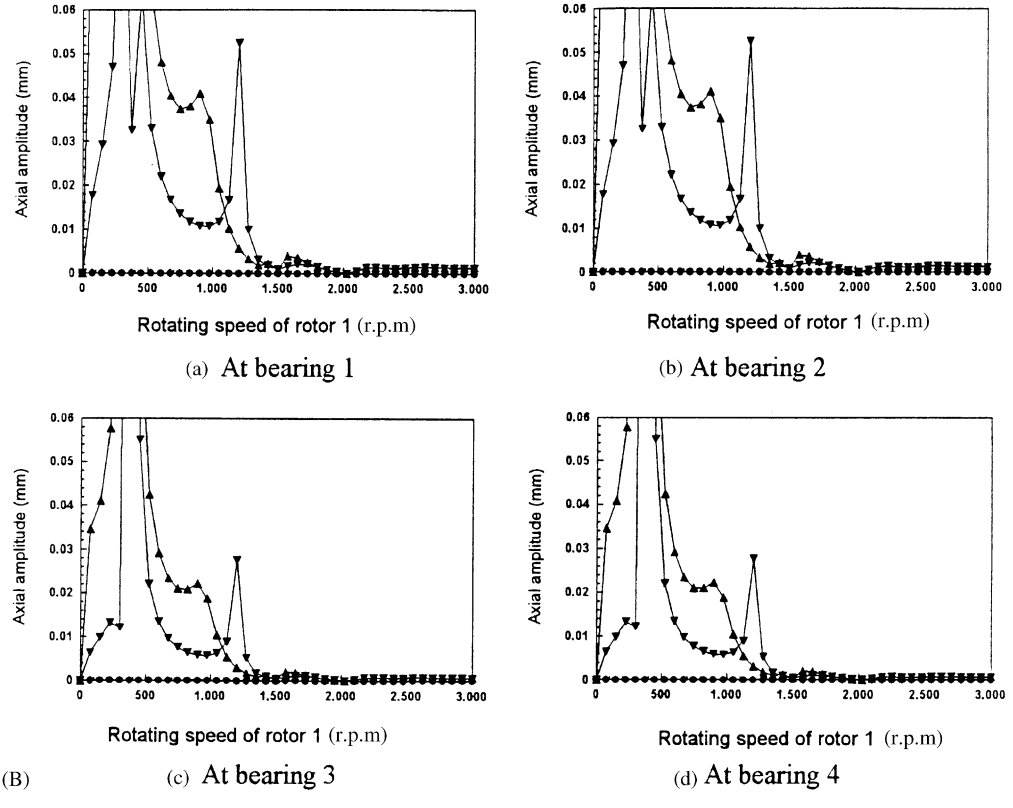

Figure 7. Continued.

represented in equation (18), where $M_0 = 100{\cdot}0\,\mathrm{N\,m}$ also acting on the bevel gear of rotor 1 and $n = 1$. The effects of the responses to the above stiffnesses are prominent under the concerned rotating speeds except the higher ones. The reason is that the number of critical speeds increases after adding the stiffnesses k_a, k_t, and the additional ones occur in the lower speeds in the analysis. We can imagine that some suitable boundary conditions may produce critical speeds in the analysis. We can imagine that some suitable boundary conditions may produce critical speeds in the higher speeds, which may greatly affect the responses at the concerned rotating speed. Consequently, during the design of this system, the dynamic characteristics of the system must be analyzed carefully. In addition, from this figure we can also find that the resonances of the system in the lateral and axial directions are excited by torsional excitation besides its own direction.

5. CONCLUSION

The model proposed in this paper to investigate the coupled axial–lateral–torsional vibration of spiral bevel-geared rotor-bearing system takes into account the constraint equation which depicts the relationship between generalized displacement of spiral bevel gear pairs, and based on it the mechanism of the coupled vibration is explained with a simplified system. The numerical analysis shows that the dynamics of the spiral bevel-geared rotor system such as the critical speeds in rigid journal supports, stability threshold speed and unbalanced responses in hydrodynamic journal bearings are not essentially

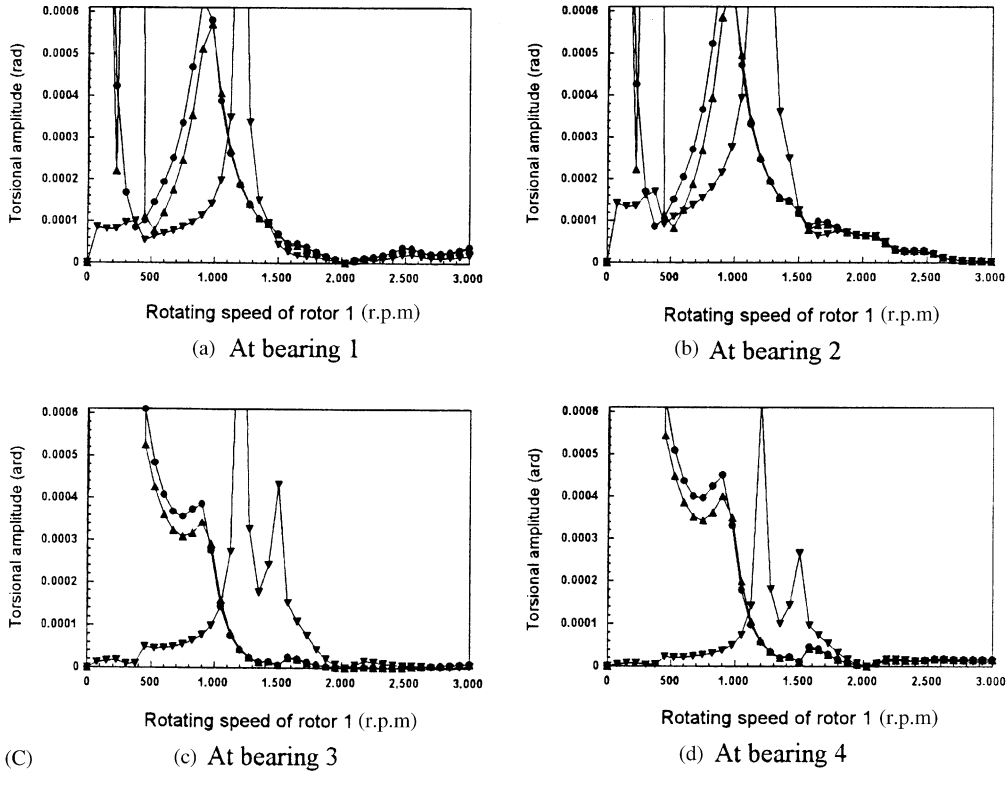

Figure 7. Continued.

different from the spur geared one. Nevertheless, the dynamic effects on boundary conditions are remarkable in comparison with the rigid supports; for instance, additional critical speeds are produced after considering the effect of axial and torsional stiffness on the ends of the rotors. Meanwhile, the investigation on the steady state response due to the torsional excitation is also presented in this paper. The consequences indicate that it can evoke considerable responses in the lateral and axial directions besides its own direction, therefore the traditional criteria for the control of vibration of the system are facing a challenge in the spiral bevel-geared rotor system.

APPENDIX A: AN EXAMPLE OF SPIRAL BEVEL-GEARED SYSTEM

In order to illustrate the modelling procedure of a spiral bevel-geared rotor system, a simple example is given here. The system is composed of two rigid bevel gears, and two massless rotors, which are supported on rigid bearings as shown in Figure 1(a). The co-ordinate systems $o_i x_i y_i z_i$ $(i = 1, 2)$ refer to rotor 1 and rotor 2, respectively, where $o_i x_i z_i$ $(i = 1, 2)$ are the horizontal planes.

For the system, equation (5) can be written as

$$\theta_2 = [d_1\theta_1 + (a_1x_1 + b_1y_1 + c_1z_1) - (a_2x_2 + b_2y_2 + c_2z_2)]/d_2. \tag{A1}$$

Kinetic energy: The total kinetic energy of the system is the summation of the translational and rotational kinetic energies of rigid disks, gears and rotors as below. After

neglecting the terms of higher order, the kinetic energy can be approximated as

$$T \approx \sum_{i=1}^{2}\left[\frac{1}{2}m_i(\dot{x}_i^2+\dot{y}_i^2+\dot{z}_i^2)+\frac{1}{2}J_i^z(\Omega_i+\dot{\theta}_i)^2+\frac{1}{2}J_i^d(\dot{\varphi}_i^2+\dot{\psi}_i^2)-J_i^z\Omega\varphi_i\dot{\psi}_i\right], \tag{A2}$$

where m_i $(i=1,2)$ is the mass of the ith gear, J_i^j $(i=1,2;\ j=d,z)$ the diametrical and polar moments of inertia, x_i, y_i, z_i, φ_i, ψ_i and θ_i $(i=1,2)$ the translational displacements of the gear center and the tilting angles, and torsional angle of the ith gear respectively.

Potential energy: The potential energy of the system results from the lateral, torsional and axial deformations:

$$U = U_l + U_t + U_a, \tag{A3}$$

where

$$\begin{aligned}U_l =& \frac{1}{2}\frac{12EI_1}{l_1^3}x_1^2-\frac{6EI_1}{l_1^2}x_1\varphi_1+\frac{1}{2}\frac{4EI_1}{l_1}\varphi_1^2+\frac{1}{2}\frac{12EI_1}{l_1^3}y_1^2-\frac{6EI_1}{l_1^2}y_1\psi_1+\frac{1}{2}\frac{4EI_1}{l_1}\psi_1^2\\ &+\frac{1}{2}\frac{12EI_2}{l_2^3}x_2^2+\frac{6EI_2}{l_2^2}x_2\varphi_2+\frac{1}{2}\frac{4EI_2}{l_2}\varphi_2^2+\frac{1}{2}\frac{12EI_2}{l_2^3}y_2^2+\frac{6EI_2}{l_2^2}y_2\psi_2+\frac{1}{2}\frac{4EI_2}{l_2}\psi_2^2,\end{aligned} \tag{A4}$$

$$U_t = \sum_{i=1}^{2}\frac{1}{2}\frac{GI_i^z}{l_i}\theta_i^2 \tag{A5}$$

and

$$U_a = \sum_{i=1}^{2}\frac{1}{2}\frac{EA_i}{l_i}z_i^2. \tag{A6}$$

In the above expressions, the mesh stiffness is not taken into account since it is much higher than the stiffness of shafts in large-scale geared rotor systems. Substitute constraint equation (A1) into expressions (A2), (A3) to eliminate θ_2 and then employ Lagrange's equation (7), where the generalized co-ordinates $q=\{x_1,y_1,z_1,\varphi_1,\psi_1,\theta_1,x_2,y_2,z_2,\varphi_2,\psi_2\}^{\mathrm{T}}$, in which there are 11 degrees of freedom in total.

Finally, we can obtain the governing equations of the system as

$$\begin{bmatrix}\mathbf{M_{11}} & \mathbf{M_{12}}\\ \mathbf{M_{21}} & \mathbf{M_{22}}\end{bmatrix}\begin{Bmatrix}\ddot{\mathbf{X}}_\mathbf{1}\\ \ddot{\mathbf{X}}_\mathbf{2}\end{Bmatrix}+\begin{bmatrix}\mathbf{G_{11}} & \mathbf{0}\\ \mathbf{0} & \mathbf{G_{22}}\end{bmatrix}\begin{Bmatrix}\dot{\mathbf{X}}_\mathbf{1}\\ \dot{\mathbf{X}}_\mathbf{2}\end{Bmatrix}+\begin{bmatrix}\mathbf{K_{11}} & \mathbf{K_{12}}\\ \mathbf{K_{21}} & \mathbf{K_{22}}\end{bmatrix}\begin{Bmatrix}\mathbf{X}_\mathbf{1}\\ \mathbf{X}_\mathbf{2}\end{Bmatrix}=0, \tag{A7}$$

where

$$\mathbf{X_1}=\{x_1\ \ y_1\ \ z_1\ \ \varphi_1\ \ \psi_1\ \ \theta_1\}^{\mathrm{T}},\qquad \mathbf{X_2}=\{x_2\ \ y_2\ \ z_2\ \ \varphi_2\ \ \psi_2\ \ \theta_2\}^{\mathrm{T}}, \tag{A8}$$

$$\mathbf{M_{11}}=\frac{1}{d_2^2}\begin{bmatrix}d_2^2m_1+a_1^2m_e & a_1b_1m_e & a_1c_1m_e & 0 & 0 & a_1d_1m_e\\ & d_2^2m_1+b_1^2m_e & b_1c_1m_e & 0 & 0 & b_1d_1m_e\\ & & d_2^2m_1+c_1^2m_e & 0 & 0 & c_1d_1m_e\\ & symm. & & d_2^2J_1^d & 0 & 0\\ & & & & d_2^2J_1^d & 0\\ & & & & & d_2^2J_1^z+d_1^2m_e\end{bmatrix}, \tag{A9}$$

$$\mathbf{M_{12}} = \mathbf{M_{21}^{T}} = -\frac{1}{d_2^2}\begin{bmatrix} a_1a_2m_e & a_1b_2m_e & a_1c_2m_e & 0 & 0 & 0 \\ a_2b_1m_e & b_1b_2m_e & b_1c_2m_e & 0 & 0 & 0 \\ a_2c_1m_e & b_2c_1m_e & c_1c_2m_e & 0 & 0 & 0 \\ 0 & 0 & 0 & 0 & 0 & 0 \\ 0 & 0 & 0 & 0 & 0 & 0 \\ a_2d_1m_e & b_2d_1m_e & c_2d_1m_e & 0 & 0 & 0 \end{bmatrix}, \tag{A10}$$

$$\mathrm{M}_{22} = \frac{1}{d_2^2}\begin{bmatrix} d_2^2m_2 + a_2^2m_e & a_2b_2m_e & a_2c_2m_e & 0 & 0 & 0 \\ & d_2^2m_2 + b_2^2m_e & b_2c_2m_e & 0 & 0 & 0 \\ & & d_2^2m_2 + c_2^2m_e & 0 & 0 & 0 \\ & \textit{symm.} & & d_2^2J_2^d & 0 & 0 \\ & & & & d_2^2J_2^d & 0 \\ & & & & & 0 \end{bmatrix}, \tag{A11}$$

$$\mathbf{G_{11}} = \begin{bmatrix} 0 & 0 & 0 & 0 & 0 & 0 \\ 0 & 0 & 0 & 0 & 0 & 0 \\ 0 & 0 & 0 & 0 & 0 & 0 \\ 0 & 0 & 0 & 0 & J_1^z\Omega_1 & 0 \\ 0 & 0 & 0 & -J_1^z\Omega_1 & 0 & 0 \\ 0 & 0 & 0 & 0 & 0 & 0 \end{bmatrix}, \quad \mathbf{G_{22}} = \begin{bmatrix} 0 & 0 & 0 & 0 & 0 & 0 \\ 0 & 0 & 0 & 0 & 0 & 0 \\ 0 & 0 & 0 & 0 & 0 & 0 \\ 0 & 0 & 0 & 0 & J_2^z\Omega_2 & 0 \\ 0 & 0 & 0 & -J_2^z\Omega_2 & 0 & 0 \\ 0 & 0 & 0 & 0 & 0 & 0 \end{bmatrix}, \tag{A12}$$

$$\mathbf{K_{11}} = \begin{bmatrix} \frac{12EI_1}{l_1^3} & 0 & 0 & -\frac{6EI_1}{l_1^2} & 0 & 0 \\ & \frac{12EI_1}{l_1^3} & 0 & 0 & -\frac{6EI_1}{l_1^2} & 0 \\ & & \frac{EA_1}{l_1} & 0 & 0 & 0 \\ & \textit{symm.} & & \frac{4EI_1}{l_1} & 0 & 0 \\ & & & & \frac{4EI_1}{l_1} & 0 \\ & & & & & \frac{GI_1^z}{l_1} \end{bmatrix}$$

$$+ k_e\begin{bmatrix} a_1^2 & a_1b_1 & a_1c_1 & 0 & 0 & a_1d_1 \\ & b_1^2 & b_1c_1 & 0 & 0 & b_1d_1 \\ & & c_1^2 & 0 & 0 & c_1d_1 \\ & & & 0 & 0 & 0 \\ & \textit{symm.} & & & 0 & 0 \\ & & & & & d_1^2 \end{bmatrix} \tag{A13}$$

$$\mathbf{K_{12}} = \mathbf{K_{21}^{T}} = -k_e \begin{bmatrix} a_1a_2 & a_1b_2 & a_1c_2 & 0 & 0 & 0 \\ a_2b_1 & b_1b_2 & b_1c_2 & 0 & 0 & 0 \\ a_2c_1 & b_2c_1 & c_1c_2 & 0 & 0 & 0 \\ 0 & 0 & 0 & 0 & 0 & 0 \\ 0 & 0 & 0 & 0 & 0 & 0 \\ a_2d_1 & b_2d_1 & c_2d_1 & 0 & 0 & 0 \end{bmatrix}, \tag{A14}$$

$$\mathbf{K_{22}} = \begin{bmatrix} \frac{12EI_2}{l_2^3} & 0 & 0 & \frac{6EI_2}{l_2^2} & 0 & 0 \\ & \frac{12EI_2}{l_2^3} & 0 & 0 & \frac{6EI_2}{l_2^2} & 0 \\ & & \frac{EA_2}{l_2} & 0 & 0 & 0 \\ & symm. & & \frac{4EI_2}{l_2} & 0 & 0 \\ & & & & \frac{4EI_2}{l_2} & 0 \\ & & & & & 0 \end{bmatrix}$$
$$+ k_e \begin{bmatrix} a_2^2 & a_2b_2 & a_2c_2 & 0 & 0 & 0 \\ & b_2^2 & b_2c_2 & 0 & 0 & 0 \\ & & c_2^2 & 0 & 0 & 0 \\ & & & 0 & 0 & 0 \\ & symm. & & & 0 & 0 \\ & & & & & 0 \end{bmatrix}, \tag{A15}$$

where $m_e = J_2^z/d_2^2$, $k_e = GI_2^z/d_2^2 l_2$.

If the oil film forces of journal bearings are considered, and the eight stiffness and damping coefficients are introduced in the related terms, we can write its differential equations as shown in equation (8).

REFERENCES

1. D. G. Lewicki, R. F. Handschuh, Z. S. Henry and F . L. Lituin 1994 *Journal of Propulsion and Power* **10**, 356–361. Low-noise, high-strength, spiral-bevel gears for helicopter transmissions.
2. T. Hirogaki, E. Aoyama, U. Yasuhiro, K. Hashimoto, K. Nitta and N. Arai 1996 *Japan Society of Mechanical Engineers, Part C* **62**, 1998–2004. Study on dynamic behavior of the Oerlikon-type spiral bevel gears (rotational vibration of gears under running conditions).
3. L. Z. Xu, M. Zhao, P. Z. Ren and W. D. Chai 1997 Jixie Kexue Yu Jishu/*Mechanical Science and Technology* **16**, 668–673. Method for analyzing the vibration behavior of rotor with the engagement of spiral bevel gears.
4. Z. G. Li, H. Y. Yang, P. Z. Ren, D. M. Wei, M. H. Wang and B. G. Hu 1998 Tuijin Jishu/*Journal of Propulsion Technology* **19**, 40–44. Calculation and analysis of vibration characteristics of a miniature engine.
5. A. Cardona 1997 *International Journal for Numerical Methods in Engineering* **40**, 357–381. Three dimensional gears modelling in multibody systems analysis.
6. Z. D. Fang, P. Gao and L. M. Song 1994 *Acta Aeronautica et Astronautica Sinica* **15**, 576–581. Vibration analysis in transmission of spiral bevel gears.

7. R. HARRIS 2000 *Shock and Vibration Digest* **32**, 22. Induced problem in a gearbox.
8. M. LI, H. Y. HU, P. L. JIANG and L. YU 2002 *Journal of Sound and Vibration* **254**, 427–446. Coupled axial–lateral–torsional dynamics of a rotor-bearing system geared by spur bevel gears.
9. Y. C. TSAI and P. C. CHIN 1987 *Transactions of the American Society of Mechanical Engineers, Journal of Mechanisms, Transmissions, and Automation in Design* **109**, 443–449. Surface geometry of straight and spiral bevel gears.
10. T. S. ZHENG, W. M. LIU and Z. B. CAI 1989 *Computers & Structures* **33**, 1139–1143. A generalized inverse iteration method for solution of quadratic eigenvalues problems in structural dynamic analysis.
11. J. S. RAO, T. N. SHIAU and J. R. CHANG 1998 *Mechanism and Machine Theory* **33**, 761–783. Theoretical analysis of lateral response due to torsional excitation of geared rotors.

APPENDIX B: NOMENCLATURE

a, b, c, d	parameters determining the geometry of gears
$\mathbf{A}$	vector of amplitudes
A	cross-sectional area of rotors
c	damping coefficient
d	diameter of rotors
D_0	diameter of bearings
E	Young's modulus
$\mathbf{G}$	gyroscopic matrix
G	shear modulus
I, I^z	second moment and polar second moment of area
J^d, J^z	diametral and polar moments of inertia of masses
k	stiffness coefficient
l	Length of rotors
L_0	length of bearings
m	mass
$\mathbf{M}, \mathbf{C}, \mathbf{K}$	generalized mass, damping and stiffness matrices
M, M_0	torque and amplitude of exciting torque
n	order number of cyclic speed
N	integer multiple of rotating speed
$\mathbf{Q}$	generalized force vector
$\mathbf{q}$	generalized displacement vector
r	radii of gears
t	time
T	kinetic energy
U	potential energy
x, y, z	co-ordinates of the lumped mass centers
α	pressure angle of gear
β	mid-spiral angle of the bevel gears
δ_1, δ_2	pitch cone angles of gear 1 and gear 2
φ, ψ, θ	tilting angles and torsional angle of the lumped mass
ψ_0, μ	clearance ratio and dynamic viscosity of bearings
Ω	rotating speed
ω	natural frequency

Subscripts

a, l, t	axial, lateral and torsional directions
b	base circle
1,2	gears (or rotors) 1 and 2
x, y	x and y components in lateral direction
R, I	real and imaginary parts of a complex number

Superscripts

d, z	diameter and the z (or polar) direction
$\dot{}, \ddot{}$	first and second order derivatives with time